Screening for CRISPR/Cas9-induced mutations using a co-injection marker in the nematode *Pristionchus pacificus*

Ken-ichi Nakayama[1], Yuuki Ishita[2], Takahiro Chihara[1, 2, 3], Misako Okumura[1, 2, 3, *]

[1]Program of Biomedical Science, Graduate School of Integrated Sciences for Life, Hiroshima University, 1-3-1 Kagamiyama, Higashi-Hiroshima, Hiroshima 739-8526, Japan

[2]Department of Biological Science, Graduate School of Science, Hiroshima University, 1-3-1 Kagamiyama, Higashi-Hiroshima, Hiroshima 739-8526, Japan

[3]Program of Basic Biology, Graduate School of Integrated Sciences for Life, Hiroshima University, 1-3-1 Kagamiyama, Higashi-Hiroshima, Hiroshima 739-8526, Japan

*Corresponding author: Misako Okumura, E-mail: okumuram@hiroshima-u.ac.jp

ORCID Takahiro Chihara: 0000-0001-9989-3619, Misako Okumura: 0000-0003-3162-0416

Acknowledgments

We would like to thank Dr. Keisuke Nakajima (Institute for Amphibian Biology, Hiroshima University) and Mr. Nobuo Yamaguchi (Natural Science Center for Basic Research and Development, Hiroshima University) for helping with microchip electrophoresis. We also thank all the members of Chihara laboratory for their kind support and Editage (www.editage.jp) for English language editing.

Funding

This work was supported by JSPS KAKENHI Grant Number 18K14716 to M.O. and 18H05369 to T.C. This work was also supported by Tomizawa Jun-ichi & Keiko Fund of Molecular Biology Society of Japan for Young Scientist and AMED under Grant Number JP19gm6310003 to M. O., and Toray Science Foundation, The Frontier Development Program for Genome Editing, and Program for Advancing Strategic International Networks to Accelerate the Circulation of Talented Researchers JPMXS05S2900002 to T.C.

Conflict of Interest: The authors declare that they have no conflict of interest.

Abstract

CRISPR/Cas9 genome editing methods are used to reveal functions of genes and molecular mechanisms underlying biological processes in many species, including nematodes. In evolutionary biology, the nematode *Pristionchus pacificus* is a satellite model and has been used to understand interesting phenomena such as phenotypic plasticity and self-recognition. In *P. pacificus*, CRISPR/Cas9-mediated mutations are induced by microinjecting a guide RNA (gRNA) and Cas9 protein into the gonads. However, mutant screening is laborious and time-consuming due to the absence of visual markers. In this study, we established a Co-CRISPR strategy by using a dominant roller marker in *P. pacificus*. We found that heterozygous mutations in *Ppa-prl-1* induced the roller phenotype, which can be used as an injection marker. After the co-injection of *Ppa-prl-1* gRNA, target gRNA, and the Cas9 protein, roller progeny and their siblings were examined using the Heteroduplex Mobility Assay and DNA sequencing. We found that some of the roller and non-roller siblings had mutations at the target site. We used varying Cas9 concentrations and found that a higher concentration of Cas9 did not increase genome-editing events. The Co-CRISPR strategy promotes the screening for genome-editing events and will facilitate the development of new genome-editing methods in *P. pacificus*.

Keywords

Pristionchus pacificus, CRISPR/Cas9, Co-injection marker, Microchip electrophoresis

Introduction

Technologies involving site-specific alteration of genomes have been developing rapidly and have enabled us to understand the function and expression of genes. Genome editing methods such as Zinc-finger nuclease, TALEN, and CRISPR/Cas9 systems have been used in a wide range of model and non-model species (Gaj et al. 2013). The CRISPR/Cas9 system is a part of the adaptive immune system in bacteria and archaea (Wiedenheft et al. 2012). It is composed of an RNA-guided DNA endonuclease (Cas9) and a guide RNA (gRNA, a complex of crRNA and tracrRNA) with a 20-bp target specific sequence (Jinek et al. 2012). The gRNA directs the Cas9 to the target sequence, and Cas9 induces double-strand breaks in DNA at the target site. The double-strand breaks are repaired by Non-Homologous End Joining (NHEJ) or Homology-Directed Repair mechanism (HDR) (Hsu et al. 2014). The NHEJ repair mechanism results in insertions and deletions (indels) while the HDR mechanism can induce Single Nucleotide Polymorphism (SNPs) or insert exogenous genes with the help of a repair template. The HDR mechanism has been used to knock-in genes of interest, such as genes encoding fluorescent proteins, within the genome of target animals (Jinek et al. 2012, 2013; Cong et al. 2013; Mali et al. 2013).

In *Caenorhabditis elegans*, the CRISPR/Cas9 system has been used for gene knock-out and knock-

in experiments (Cho et al. 2013; Tzur et al. 2013; Chiu et al. 2013; Chen et al. 2013; Dickinson et al. 2013; Lo et al. 2013). When using the CRISPR/Cas9 system for genome editing, plasmids expressing gRNA and Cas9 or an *in-vitro* assembled gRNA-Cas9 complex (Ribonucleoprotein complex, RNP complex) are injected into the gonads of adult animals via microinjection. To check mutations at the target sites, Sanger sequencing or high resolution melting analysis are used for all F1 progeny (Wittwer, 2009; Vossen et al. 2009; Cho et al. 2013; Samarut et al. 2016). Thus, generating mutants via the CRISPR/Cas9 system is a time-consuming and costly process. Recently, a Co-CRISPR strategy has been utilized to screen genome-edited animals (Arribere et al. 2014; Kim et al. 2014). In this method, a gRNA, as an injection marker, is co-injected with a gRNA as the gene of interest. For the Co-CRISPR marker, genes such as *Cel-rol-6*, *Cel-unc-58*, and *Cel-dpy-10* have been used, as they exhibit obvious morphological or behavioral phenotypes in heterozygous mutants (Brenner, 1974; Park & Horvitz, 1986; Levy et al. 1993). These F1 mutants often have mutations in the target locus. Therefore, the Co-CRISPR strategy is a powerful way to screen genome-edited events in *C. elegans* (Arribere et al. 2014; Kim et al. 2014).

In evolutionary biology, the diplogastrid nematode *Pristionchus pacificus* has been established as a satellite model organism for comparison with *C. elegans* (Sommer et al. 1996, 2015). *P. pacificus* is a self-fertilizing hermaphrodite and can be cultured on *Escherichia coli* OP50 with a 4-day life cycle (Sommer et al. 1996). A wide range of biological discoveries in the fields of evolution, development,

neurobiology, and genomics have been revealed using *P. pacificus* (Eizinger & Sommer, 1997; Dieterich et al., 2008; Hong et al. 2008; Bento et al. 2010; Bose et al. 2012; Bumbarger et al. 2013; Ragsdale et al. 2013; Wilecki et al. 2015). Various genetic tools have been developed, including whole genome sequencing (Dieterich et al. 2008), genetic transformation (Schlager et al. 2009), and microparticle bombardment (Namai and Sugimoto 2018). Gene inactivation using the CRISPR/Cas9 system has also been established in *P. pacificus* (Witte et al. 2015). Microinjection of gRNA-Cas9 complex (RNP complex) into the gonads induces mutagenesis in F1 animals. This powerful genome-editing method has been widely used in *P. pacificus* to understand the mechanisms of various phenomena such as phenotypic plasticity, feeding behavior, self-recognition, sensory system, and evolution (Mayer et al. 2015; Serobyan et al. 2016; Okumura et al. 2017; Moreno et al. 2019; Sieriebriennikov et al. 2017; Falcke et al. 2018; Namdeo et al. 2018; Lightfoot et al. 2019). However, because of the lack of injection markers in *P. pacificus*, it is difficult and time-consuming to find the target mutants or knock-in alleles. Therefore, establishing a Co-CRISPR strategy in *P. pacificus* to screen for CRISPR-mediated mutations easily is an urgent requirement.

Here, using *Ppa-prl-1* as a Co-CRISPR injection marker, we established the Co-CRISPR strategy in *P. pacificus*. We demonstrated that CRISPR-induced mutations in *Ppa-prl-1*, encoding cuticle collagen, led to a dominant roller phenotype. We found that some of the roller mutants and their siblings also had mutations in the target locus. We propose that this strategy will improve the screening efficiency

of CRISPR-mediated mutants in *P. pacificus*.

Materials and Methods

Worm Strain

All experiments were performed using the *P. pacificus* laboratory wild-type strain PS312 (Sommer et al. 1996; Sommer and Sternberg, 1996). *P. pacificus* was maintained at 20 ℃ on NGM agar plates with *Escherichia coli* OP50 as described previously (Sommer and Sternberg, 1996).

Preparation of injection mix

To identify *P. pacificus* orthologs of *Cel-tax-2* and *Cel-tax-4*, we conducted BLAST searches against the *P. pacificus* reference genome (version El Paco, www.pristionchus.org). *Ppa-tax-2* (UMM-S13-30.6 mRNA-1) and *Ppa-tax-4* (UMA-S50-12.70 mRNA-1) were closely related to *Cel-tax-2* and *Cel-tax-4*. We designed the CRISPR target sequences using CHOP-CHOP (http://chopchop.cbu.uib.no/). The sequences of the gene-specific part of the crRNA were as follows:

Ppa-prl-1: 5'-AGAGTCCGTCGTCAATACCC-3'

Ppa-tax-2: 5'-CGTGAACAGCTGCGTATACT-3'

Ppa-tax-4: 5'-CGCTCACTCTTACTACGATT-3'

All tracrRNA and crRNA were synthesized by Integrated DNA Technologies (IDT). To make gRNA,

we mixed tracrRNA (100 μM) and crRNA (100 μM) in a 1:1 molar ratio. The mixture was incubated at 95 °C for 5 min and then at room temperature for 5 min. The gRNAs were stored at -80 °C. To make an RNP complex, a gRNA (*Ppa-tax-2*, *Ppa-tax-4 or Ppa-prl-1*) and Cas9 protein (IDT, 10 mg/ml) were mixed in a 2:1 molar ratio and incubated at 37 °C for 10 min. The target gRNAs (*Ppa-tax-2* or *Ppa-tax-4)* and the marker gRNA (*Ppa-prl-1*) were mixed with the Cas9 protein separately, and the two RNP complexes were combined to make the injection mix and diluted with nuclease-free water. The details of the amount of the co-injection mix and the concentration of Cas9 are given in Table 1.

A repair template for *Ppa-prl-1* was synthesized as single-stranded DNA by Eurofins Genomics. To avoid double-strand breaks, the repair template had silent mutations. We mixed the repair template at a final concentration of 500 nM in the injection mix. The sequence of the repair template of *Ppa-prl-1* was as follows:

5'-AGAGACGTCATCGTTCTTGGCAAGACTTCTCGCCGAGTACGCTGCCAGTATCCAGGA

GAGGAACCCTCGAACACTGGATATCCTGGTGATTTCCCTACCC-3'

Microinjection and screening for roller F1 progeny

Injection mixtures were microinjected into the gonads of adult worms. Injected worms (P0) were placed individually on NGM plates. After about 24 hours, P0 worms were discarded. After 3-4 days, F1s were screened for the roller phenotype.

Screening for mutations by Heteroduplex Mobility Assay

Roller F1s and their non-roller siblings were transferred to 96-well plates with worm lysis buffer (10 mM Tris, 50 mM KCI, 2.5 mM $MgCl_2 \cdot 6H_2O$, 0.45% Nonidet P-40, 0.45% Tween20 adjusted pH to 8.3 with HCl). Proteinase K (Takara, 9034) was added to the lysis buffer (6 µl of proteinase K to 1 ml lysis buffer). Using the lysate as a template, the regions, including the CRISPR-Cas9 target sites, were PCR-amplified with a high-fidelity DNA polymerase such as KOD One (TOYOBO, KMM-101). PCR products were 150-250-bp long and the target sites were located at the center of the PCR products. The following primers were used for PCR amplification:

Ppa-tax-2 Forward Primer: 5'-TTTTCGGCTTTGTTTCTTGAATG-3'

Ppa-tax-2 Reverse Primer: 5'-CTGGTCTTGTGATCTGGAATTG-3'

Ppa-tax-4 Forward Primer: 5'-ATCCAAATTCGATGATTTCCAG-3'

Ppa-tax-4 Reverse Primer: 5'-TGCTTTGATAAAATGCTATTCCC-3'

The PCR products were diluted 3-5-fold with Tris-EDTA Buffer (TE) or water, denatured at 95 ℃ for 5 min, and reannealed by cooling the products to 4 ℃ at the speed of 0.1 ℃/sec. The solution was analyzed using a microchip electrophoresis MultiNA (Shimazu, MCE-202) with the DNA-500 Separation Buffer and in the premix mode. Base pair fragments that were 500-600 bp long containing the target sites were amplified for Sanger sequencing (Eurofins Genomics). The following primers

were used for PCR amplification:

Ppa-prl-1 Forward Primer: 5'-ATGAAGGTCCATACGGGAGC-3'

Ppa-prl-1 Reverse Primer: 5'-CTCCAGTGGGACAATAGAAGCAAG-3'

Ppa-tax-2 Forward Primer: 5'-GTATTGCCTCATTGTCAGAGATTAGAGTGAC-3'

Ppa-tax-2 Reverse Primer: 5'-CACTTTCTCACAGAGTAGTCCTTCCCTATC-3'

Ppa-tax-4 Forward Primer: 5'-TAATCATCATTCACTGGAACGCG-3'

Ppa-tax-4 Reverse Prime: 5'-CCGACGTTACCTGAACGGAAAG-3'

The following primers were used to read the sequences:

Ppa-prl-1 Primer: 5'-CTCTCTCATTGCTTGCATGGTTCTC-3'

Ppa-tax-2 Primer: 5'-AGGTGAGATTATCGAGTCTGTTC-3'

Ppa-tax-4 Primer: 5'-TCGGATACGTGGGTTTACGGAG-3'

Statistical analysis

The Prism software package GraphPad Software 7 was used to carry out statistical analyses. Information about statistical tests, P-values, and n-numbers are provided in the legend of Figure 3.

Results and discussion

Heterozygous mutants of *Ppa-prl-1* exhibit a roller phenotype

To establish the Co-CRISPR method in *P. pacificus* (Fig. 1), we selected behavioral or morphological dominant genes that can be easily used for screening of heterozygous F1 progeny. Previous studies reported that Arginine to Cysteine mutation (R65C) in the homologous residue in *Cel-rol-6*, *Cel-sqt-1*, and *Ppa-prl-1* encoding collagen, induced a dominant roller phenotype in *C. elegans* and *P. pacificus* (Kramer & Johnson, 1993; Kenning et al. 2004; Schlager et al. 2009). To examine whether this point mutation caused the dominant roller phenotype by CRISPR/Cas9 genome editing in *P. pacificus*, we designed crRNA for *Ppa-prl-1* and a repair template containing the point mutation (Fig. 2a). From 17 injected P0 worms, we obtained 204 F1 worms, and from three P0 worms, six of them showed the roller phenotype (Fig. 2b, c). We examined the DNA sequence of *Ppa-prl-1* locus in three roller F1 progeny. One of the worms had the R65C mutation induced by the repair template (Fig. 2a, #1). Unexpectedly, the roller phenotype was also observed in worms with indels (Fig. 2a, #2, #3). These results indicate that heterozygous mutants of *Ppa-prl-1* showed the roller phenotype and the repair template for *Ppa-prl-1* was not necessary to induce the roller phenotype in *P. pacificus*.

Co-CRISPR knockout and screening for mutations using microchip electrophoresis

Ppa-prl-1 may be used as a potential Co-CRISPR marker because CRISPR-mediated mutations in *Ppa-prl-1* caused the dominant roller phenotype. To address this opportunity for a visual indicator, we co-injected the *Ppa-prl-1* gRNA with the gRNA for *Ppa-tax-2* or *Ppa-tax-4* (cGMP-gated channels)

(Table 2). Since the roller phenotype was induced without the repair template of *Ppa-prl-1* (Fig. 2), we injected both with and without the repair template for *Ppa-prl-1* (Table 2). To identify CRISPR-mediated mutations in *Ppa-tax-2*, we used Heteroduplex Mobility Assay (HMA) performed by microchip electrophoresis (Fig. 3a) (Ansai & Kinoshita, 2014). Mutations were confirmed by Sanger sequencing. We tried five conditions of the injection mix and found four mutations in *Ppa-tax*-2 out of 11 roller F1s (Table 2). This result suggested that two different gRNA injected simultaneously can induce mutations in both *Ppa-prl-1* and the target locus in *P. pacificus*. To identify more mutations in the target locus, we also examined the non-roller siblings of the roller F1s and found that 19 out of 283 (6.7%) F1s had mutations in *Ppa-tax-2* target site (Fig. 3b, c) (Table 2, 3). The rate of the genome-editing event in *Ppa-tax*-2 in non-roller siblings was less than that of the roller F1s. Similar results were obtained for *Ppa-tax-4* (Table 2, 3), suggesting that the Co-CRISPR strategy can be applied to other gene loci and *Ppa-prl-1* can be utilized as a co-injection marker. We also found that the P0 animals that produced a higher number of rollers tended to produce a higher number of mutations in the target loci (Fig. 3d). Our results revealed that when rollers have the target mutations, the probability that non-roller siblings have also the target mutations increases (Table 3). These results suggest that multiple rollers in a brood have a higher chance having the target mutations and non-rollers that have roller siblings with the target mutations are also good candidates to screen the target mutations.

Cas9 concentration affects the efficiency of genome editing events

Previous studies have shown that the Cas9-RNP complex can be toxic at high concentrations and the high RNP concentration interferes with the efficiency of on-target genome editing in *C. elegans* (Dokshin et al. 2018). Therefore, we tried different Cas9 concentrations (0.25 μg/μl・0.5 μg/μl・0.62 μg/μl) in *P. pacificus* (Table 2). A single injection of 0.62 μg/μl Cas9 and the repair template produced the highest number of roller F1s, however, the average of the total number of F1s was decreased when 0.62 μg/μl Cas9 was injected (Fig. 3e). The Cas9 concentration did not affect the number of rollers per injected animals, but the injection of the lower concentrations of Cas9 tended to induce the largest number of mutations in *Ppa-tax-2* and *Ppa-tax4* (Table 3). These results suggest that the high Cas9 concentration could be toxic for *P. pacificus* and the 0.25 μg/μl Cas9 protein was enough to perform the Co-CRISPR strategy.

Conclusion

The CRISPR/Cas9 genome editing methods have changed biological research but finding successful genome-editing events is still time-consuming and laborious. To overcome this difficulty, we established the Co-CRISPR strategy in *P. pacificus* using *Ppa-prl-1* as the dominant co-injection marker. This method can be used to make CRISPR-knockout mutants for various genes. Other injection markers located on other chromosomes may be necessary to choose more suitable markers

for different target genes. The Co-CRISPR strategy promotes the easy screening of genome-edited worms to facilitate future studies using the model *P. pacificus*.

Figure Legends

Fig. 1 Method of Co-CRISPR

Schematic representation of the Co-CRISPR method in *P. pacificus*. Pre-assembled gRNA of the dominant co-injection marker *Ppa-prl-1*/Cas9 complexes are co-injected with pre-assembled a target gRNA-Cas9 complexes. Then, roller F1s and their siblings are isolated and screened for indels by Heteroduplex Mobility Assay (HMA) and Sanger sequencing. Orange worms indicate heterozygous mutants of the target gene.

Fig. 2 Mutations in *Ppa-prl-1* induce the roller phenotype

a: DNA Sequences of wild type, the repair template, and roller mutants in *Ppa-prl-1*. The sequence of the repair template was altered for avoiding double-strand breaks. Red and blue boxes indicate Protospacer Adjacent Motif (PAM) and the Cas9 target site of the gRNA, respectively. Deletions (-) and insertions (+) are indicated to the right of each mutated sequence. Small letters indicate insertions.

b, c: Image of wild type (b) and *Ppa-prl-1* mutant (c) with the roller phenotype.

Fig. 3 Co-CRISPR mutagenesis in *Ppa-tax-2* and *Ppa-tax-4*

a: The Heteroduplex Mobility Assay (HMA). The region including the mutated locus is amplified by PCR. The denatured and annealed PCR products of heterozygous mutants form a heteroduplex and the differences in their mobility can be detected by the microchip electrophoresis.

b: The representative result of HMA in the wild type, an F1 roller, and non-roller siblings injected with a mixture containing 0.25 μg/μl Cas9 protein without a repair template. While the PCR product of the wild type gives a clear single band, the PCR products of the F1 roller and the non-roller siblings form a heteroduplex and result in multiple bands.

c: The target sequence of *Ppa-tax-2* locus in the roller and the non-roller siblings. Red and blue boxes indicate PAM and the target site of the gRNA, respectively. The number of deletions (-) is indicated to the right of each mutated sequence.

d: Scatter plot of the number of rollers born from the same mother vs the number of *Ppa-tax-2* or *Ppa-tax-4* mutants born from the same mother. Y-axis indicates the sum of the mutants in the target loci in rollers and non-roller siblings.

e: The number of total F1s derived from P0 injected with the different Cas9 concentrations. Data of *Ppa-tax-2* and *Ppa-tax-4* were merged. 0.25 μg/μl, n = 84; 0.5 μg/μl, n = 74; 0.62 μg/μl, n = 79. Error bars are SEM. One-way ANOVA, Tukey's multiple comparison tests. *$p < 5.0 \times 10^{-2}$, ****$p < 1.0 \times 10^{-4}$; n.s, not significant.

Table 1 Composition of the co-injection mix

Table 2 Summary of the Co-CRISPR method of *Ppa-prl-1* and *Ppa-tax-2* or *Ppa-tax-4*

Table 3 Individual results of P0 animals that produced rollers

We numbered P0 animals that produced rollers for each Cas9 condition.

References

Ansai, S., & Kinoshita, M. (2014). Targeted mutagenesis using CRISPR/Cas system in medaka. *Biology Open*, *3*(5), 362–371. https://doi.org/10.1242/bio.20148177

Arribere, J. A., Bell, R. T., Fu, B. X. H., Artiles, K. L., Hartman, P. S., & Fire, A. Z. (2014). Efficient Marker-Free Recovery of Custom Genetic Modifications with CRISPR/Cas9 in Caenorhabditis elegans. *Genetics*, *198*, 837–846. https://doi.org/10.1534/genetics.114.169730

Bento, G., Ogawa, A., & Sommer, R. J. (2010). Co-option of the hormone-signalling module dafachronic acid-DAF-12 in nematode evolution. *Nature*, *466*(7305), 494–497. https://doi.org/10.1038/nature09164

Bose, N., Ogawa, A., von Reuss, S. H., Yim, J. J., Ragsdale, E. J., Sommer, R. J., & Schroeder, F. C.

(2012). Complex Small-Molecule Architectures Regulate Phenotypic Plasticity in a Nematode. *Angewandte Chemie International Edition*, *51*(50), 12438–12443. https://doi.org/10.1002/anie.201206797

Brenner, S. (1974). THE GENETICS OF CAENORHABDZTZS ELEGANS. *Genetics*, *77*(1), 71–94. Retrieved from http://www.genetics.org/content/genetics/77/1/71.full.pdf

Bumbarger, D. J., Riebesell, M., Rödelsperger, C., & Sommer, R. J. (2013). System-wide rewiring underlies behavioral differences in predatory and bacterial-feeding nematodes. *Cell*, *152*(1–2), 109–119. https://doi.org/10.1016/j.cell.2012.12.013

Chen, C., Fenk, L. A., & De Bono, M. (2013). Efficient genome editing in *Caenorhabditis elegans* by CRISPR-targeted homologous recombination. *Nucleic Acids Research*, *41*(20). https://doi.org/10.1093/nar/gkt805

Chiu, H., Schwartz, H. T., Antoshechkin, I., & Sternberg, P. W. (2013). Transgene-free genome editing in *Caenorhabditis elegans* using CRISPR-Cas. *Genetics*, *195*(3), 1167–1171. https://doi.org/10.1534/genetics.113.155879

Cho, S. W., Lee, J., Carroll, D., Kim, J. S., & Lee, J. (2013). Heritable gene knockout in *Caenorhabditis elegans* by direct injection of Cas9-sgRNA ribonucleoproteins. *Genetics*, *195*(3), 1177–1180. https://doi.org/10.1534/genetics.113.155853

Dieterich, C., Clifton, S. W., Schuster, L. N., Chinwalla, A., Delehaunty, K., Dinkelacker, I., … Sommer,

R. J. (2008). The *Pristionchus pacificus* genome provides a unique perspective on nematode lifestyle and parasitism. *Nature Genetics*, *40*(10), 1193–1198. https://doi.org/10.1038/ng.227

Dokshin, G. A., Ghanta, K. S., Piscopo, K. M., & Mello, C. C. (2018). Robust Genome Editing with Short Single-Stranded. *GENETICS*, *210*(November), 781–787.

Eizinger, A., & Sommer, R. J. (1997). The homeotic gene *lin-39* and the evolution of nematode epidermal cell fates. *Science*, *278*(5337), 452–455. https://doi.org/10.1126/science.278.5337.452

Falcke, J. M., Bose, N., Artyukhin, A. B., Rödelsperger, C., Markov, G. V., Yim, J. J., … Sommer, R. J. (2018). Linking Genomic and Metabolomic Natural Variation Uncovers Nematode Pheromone Biosynthesis. *Cell Chemical Biology*, *25*(6), 787–796. https://doi.org/10.1016/j.chembiol.2018.04.004

Gaj, T., Gersbach, C. A., & Barbas, C. F. (2013). ZFN, TALEN, and CRISPR/Cas-based methods for genome engineering. *Trends in Biotechnology*. https://doi.org/10.1016/j.tibtech.2013.04.004

Hong, R. L., Witte, H., & Sommer, R. J. (2008). Natural variation in *Pristionchus pacificus* insect pheromone attraction involves the protein kinase EGL-4. *Proceedings of the National Academy of Sciences of the United States of America*, *105*(22), 7779–7784. https://doi.org/10.1073/pnas.0708406105

Hsu, P. D., Lander, E. S., & Zhang, F. (2014). Development and applications of CRISPR-Cas9 for genome engineering. *Cell*. https://doi.org/10.1016/j.cell.2014.05.010

Jinek, M., Chylinski, K., Fonfara, I., Hauer, M., Doudna, J. A., & Charpentier, E. (2012). A Programmable Dual-RNA–Guided DNA Endonuclease in Adaptive Bacterial Immunity. *Science*, *337*(August), 816–822.

Jinek, M., East, A., Cheng, A., Lin, S., Ma, E., & Doudna, J. (2013). RNA-programmed genome editing in human cells. *ELife*, (2), 1–9. https://doi.org/10.7554/eLife.00471

Kenning, C., Kipping, I., & Sommer, R. J. (2004). Isolation of mutations with Dumpy-like phenotypes and of collagen genes in the nematode Pristionchus pacificus. *Genesis*, *40*(3), 176–183. https://doi.org/10.1002/gene.20084

Kim, H., Ishidate, T., Ghanta, K. S., Seth, M., Conte, D., Shirayama, M., & Mello, C. C. (2014). A co-CRISPR strategy for efficient genome editing in *Caenorhabditis elegans*. *Genetics*, *197*(4), 1069–1080. https://doi.org/10.1534/genetics.114.166389

Kramer, J. M., & Johnson, J. J. (1993). Analysis of mutations in the *sqt-1* and *rol-6* collagen genes of *Caenorhabditis elegans*. *Genetics*, *135*(4), 1035–1045.

Le Cong, F. Ann Ran, David Cox, Shuailiang Lin, Robert Barretto, Naomi Habib, Patrick D. Hsu, Xuebing Wu, Wenyan Jiang, Luciano A. Marraffini, F. Z. (2013). Multiplex Genome Engineering Using CRISPR/Cas Systems. *Science*, *339*(February), 819–824.

Levy, A. D., Yang, J., & Kramer, J. M. (1993). Molecular and genetic analyses of the *Caenorhabditis elegans dpy-2* and *dpy-10* collagen genes: A variety of molecular alterations affect organismal

morphology. *Molecular Biology of the Cell*, *4*(8), 803–817. https://doi.org/10.1091/mbc.4.8.803

Lightfoot, J. W., Martin Wilecki, C. R., Moreno, E., Susoy, V., Witte, H., & Sommer, R. J. (2019). Small peptide–mediated self-recognition prevents cannibalism in predatory nematodes, *9*(April), 86–89.

Lo, T. W., Pickle, C. S., Lin, S., Ralston, E. J., Gurling, M., Schartner, C. M., … Meyer, B. J. (2013). Precise and heritable genome editing in evolutionarily diverse nematodes using TALENs and CRISPR/Cas9 to engineer insertions and deletions. *Genetics*, *195*(2), 331–348. https://doi.org/10.1534/genetics.113.155382

Mali, P., Yang, L., Esvelt, K. M., Aach, J., Guell, M., DiCarlo, J. E., … M., C. G. (2013). RNA-guided human genome engineering via Cas9. *Science*, *339*(6121), 823–826. https://doi.org/10.1126/science.1232033

Mayer, M. G., Rödelsperger, C., Witte, H., Riebesell, M., & Sommer, R. J. (2015). The Orphan Gene dauerless Regulates Dauer Development and Intraspecific Competition in Nematodes by Copy Number Variation. *PLoS Genetics*, *11*(6), 1005146. https://doi.org/10.1371/journal.pgen.1005146

Moreno, E., Lightfoot, J. W., Lenuzzi, M., & Sommer, R. J. (2019). Cilia drive developmental plasticity and are essential for efficient prey detection in predatory nematodes. *Proceedings of the Royal Society B: Biological Sciences*, *286*(1912). https://doi.org/10.1098/rspb.2019.1089

Namai, S., & Sugimoto, A. (2018). Transgenesis by microparticle bombardment for live imaging of fluorescent proteins in *Pristionchus pacificus* germline and early embryos. *Development Genes and*

Evolution, *228*(1), 75–82. https://doi.org/10.1007/s00427-018-0605-z

Namdeo, S., Moreno, E., Rödelsperger, C., Baskaran, P., Witte, H., & Sommer, R. J. (2018). Two independent sulfation processes regulate mouth-form plasticity in the nematode *Pristionchus pacificus*. *Development*, *145*(13). https://doi.org/10.1242/dev.166272

Okumura, M., Wilecki, M., & Sommer, R. J. (2017). Serotonin Drives Predatory Feeding Behavior via Synchronous Feeding Rhythms in the Nematode *Pristionchus pacificus*. *G3*, *7*, 3745–3755. https://doi.org/10.1534/g3.117.300263

Park, E. C., & Horvitz, H. R. (1986). Mutations with dominant effects on the behavior and morphology of the nematode *Caenorhabditis elegans*. *Genetics*, *113*(4), 821–852.

Ragsdale, E. J., Müller, M. R., Rödelsperger, C., & Sommer, R. J. (2013). A developmental switch coupled to the evolution of plasticity acts through a sulfatase. *Cell*, *155*(4), 922–933. https://doi.org/10.1016/j.cell.2013.09.054

Samarut, É., Lissouba, A., & Drapeau, P. (2016). A simplified method for identifying early CRISPR-induced indels in zebrafish embryos using High Resolution Melting analysis. *BMC Genomics*, *17*(1), 1–6. https://doi.org/10.1186/s12864-016-2881-1

Schlager, B., Wang, X., Braach, G., & Sommer, R. J. (2009). Molecular cloning of a dominant roller mutant and establishment of DNA-mediated transformation in the nematode *Pristionchus pacificus*. *Genesis*, *47*(5), 300–304. https://doi.org/10.1002/dvg.20499

Serobyan, V., Xiao, H., Namdeo, S., Rödelsperger, C., Sieriebriennikov, B., Witte, H., … Sommer, R. J. (2016). Chromatin remodelling and antisense-mediated up-regulation of the developmental switch gene eud-1 control predatory feeding plasticity. *Nature Communications*, *7*(12337). https://doi.org/10.1038/ncomms12337

Sieriebriennikov, B., Markov, G. V, Witte, H., & Sommer, R. J. (2017). The Role of DAF-21/Hsp90 in Mouth-Form Plasticity in *Pristionchus pacificus*. *Mol Biol Evol*, *34*(7), 1644–1653. https://doi.org/10.1093/molbev/msx106

Sommer, R., Carta, L., Kim, S.-Y., & Sternberg, P. W. S. (1996). Morphological, genetic and molecular description of *Pristionchus pacificus* sp. n. (Nematoda:Neodiplogastridae). *Fundamental and Applied Nematology*.

Sommer, R. J., & Sternberg, P. W. (1996). Apoptosis and change of competence limit the size of the vulva equivalence group in *Pristionchus pacificus*: a genetic analysis. *Current Biology*, *6*(1), 52–59. https://doi.org/10.1016/S0960-9822(02)00421-9

Tzur, Y. B., Friedland, A. E., Nadarajan, S., Church, G. M., Calarco, J. A., & Colaiácovo, M. P. (2013). Heritable custom genomic modifications in *Caenorhabditis elegans* via a CRISPR-Cas9 system. *Genetics*, *195*(3), 1181–1185. https://doi.org/10.1534/genetics.113.156075

Vossen, R. H. A. M., Aten, E., Roos, A., & Den Dunnen, J. T. (2009). High-resolution melting analysis (HRMA) - More than just sequence variant screening. *Human Mutation*, *30*(6), 860–866.

https://doi.org/10.1002/humu.21019

Wiedenheft, B., Sternberg, S. H., & Doudna, J. A. (2012). RNA-guided genetic silencing systems in bacteria and archaea. *Nature*, *482*(7385), 331–338. https://doi.org/10.1038/nature10886

Wilecki, M., Lightfoot, J. W., Susoy, V., & Sommer, R. J. (2015). Predatory feeding behaviour in *Pristionchus* nematodes is dependent on phenotypic plasticity and induced by serotonin. *The Journal of Experimental Biology*, *218*, 1306–1313. https://doi.org/10.1242/jeb.118620

Witte, H., Moreno, E., Rödelsperger, C., Kim, J., Kim, J.-S., Streit, A., & Sommer, R. J. (2015). Gene inactivation using the CRISPR/Cas9 system in the nematode *Pristionchus pacificus*. *Dev Genes Evol*, *225*, 55–62. https://doi.org/10.1007/s00427-014-0486-8

Wittwer, C. T. (2009). High-resolution DNA melting analysis: Advancements and limitations. *Human Mutation*, *30*(6), 857–859. https://doi.org/10.1002/humu.20951

Fig. 1

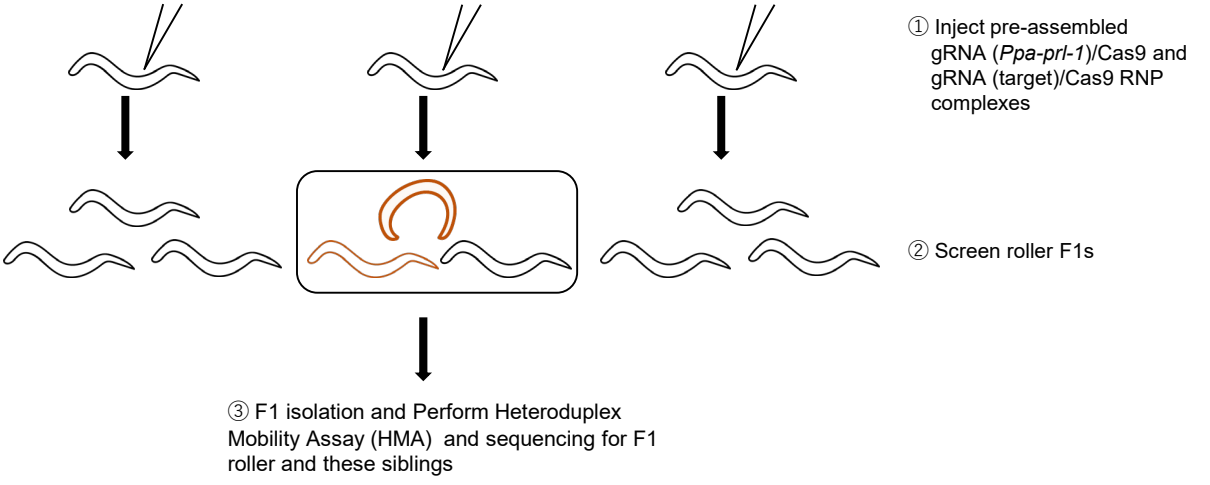
① Inject pre-assembled gRNA (*Ppa-prl-1*)/Cas9 and gRNA (target)/Cas9 RNP complexes
② Screen roller F1s
③ F1 isolation and Perform Heteroduplex Mobility Assay (HMA) and sequencing for F1 roller and these siblings

Fig. 2

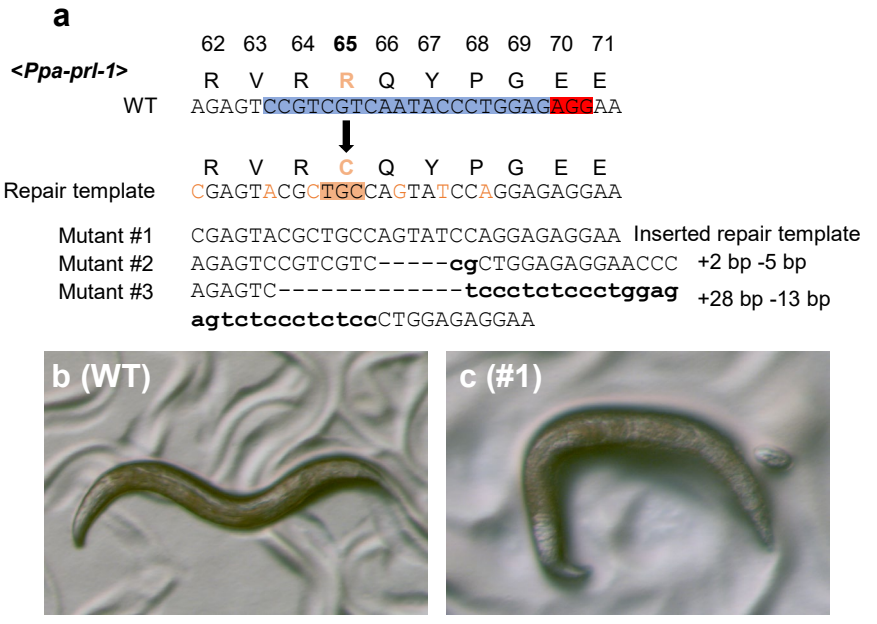
a
62 63 64 65 66 67 68 69 70 71
<Ppa-prl-1>
R V R R Q Y P G E E
WT
AGAGTCCGTCGTCAATACCCTGGAGAGGAA
R V R C Q Y P G E E
Repair template
CGAGTACGCTGCCAGTATCCAGGAGAGGAA
Mutant #1
CGAGTACGCTGCCAGTATCCAGGAGAGGAA
Inserted repair template
Mutant #2
AGAGTCCGTCGTC-----cgCTGGAGAGGAACCC
+2 bp -5 bp
Mutant #3
AGAGTC----------tccctctccctggag
+28 bp -13 bp
agtctccctctccCTGGAGAGGAA
b (WT)
c (#1)

Fig. 3

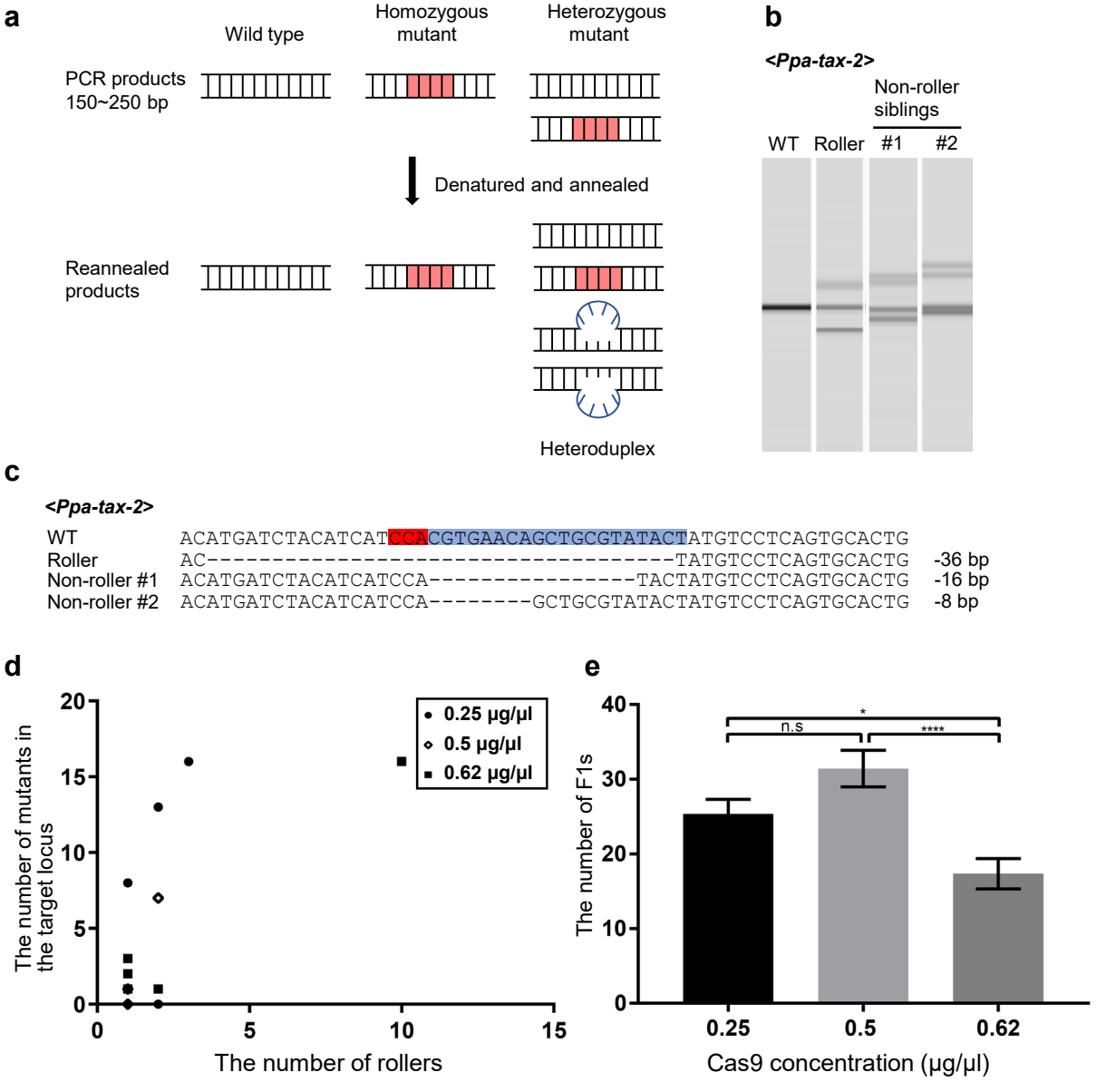
a
Wild type
Homozygous mutant
Heterozygous mutant
PCR products 150~250 bp
Denatured and annealed
Reannealed products
Heteroduplex
b
<Ppa-tax-2>
Non-roller siblings
WT
Roller
#1
#2
c
<Ppa-tax-2>
WT ACATGATCTACATCATCCACGTGAACAGCTGCGTATACTATGTCCTCAGTGCACTG
Roller AC----------TATGTCCTCAGTGCACTG -36 bp
Non-roller #1 ACATGATCTACATCATCCA----------TACTATGTCCTCAGTGCACTG -16 bp
Non-roller #2 ACATGATCTACATCATCCA--------GCTGCGTATACTATGTCCTCAGTGCACTG -8 bp
d
0.25 μg/μl
0.5 μg/μl
0.62 μg/μl
The number of mutants in the target locus
The number of rollers
e
n.s
*
****
The number of F1s
Cas9 concentration (μg/μl)
0.25
0.5
0.62

Table 1

	Ppa-tax-2 or *Ppa-tax-4*		*Ppa-prl-1*			
Cas9 concentration (µg/µl)	10 mg/ml Cas9 (µl)	gRNA (µl)	10 mg/ml Cas9 (µl)	gRNA (µl)	10 µM Repair template (µl)	Nuclease free water (µl)
0.25	0.25	0.61	0.25	0.61	1	to 20 µl
0.5	0.5	1.22	0.5	1.22		to 20 µl
0.62	0.62	1.51	0.62	1.51	1	to 20 µl

Table 2

Locus	Cas9 concentration (µg/µl)	Repair template	Number of injection	Injected animals yielding roller	F1 roller	Mutant F1/ roller F1	Mutant F1 / non-roller siblings
Ppa-tax-2	0.25	-	34	3	5	2/5 (40%)	19/166 (11.4%)
Ppa-tax-2	0.5	-	31	1	1	0/1 (0%)	0/47 (0%)
Ppa-tax-2	0.62	-	39	0	0	-	-
Ppa-tax-2	0.25	+	9	2	2	0/2 (0%)	0/56 (0%)
Ppa-tax-2	0.62	+	5	2	3	2/3 (66.7%)	0/14 (0%)
Ppa-tax-4	0.25	-	41	4	7	2/7(28.6%)	15/143 (10.5%)
Ppa-tax-4	0.5	-	43	2	3	0/3 (0%)	7/104 (6.7%)
Ppa-tax-4	0.62	-	19	1	1	0/1 (0%)	3/73 (4.1%)
Ppa-tax-4	0.62	+	16	2	11	10/11(91%)	8/51 (15.7%)

Table 3

Locus	Cas9 concentration (μg/μl)	Repair template	P0 number	Total F1	F1 roller	Mutant F1/ roller F1	Mutant F1 / non-roller siblings
Ppa-tax-2	0.25	-	①	69	2	1/2 (50%)	12/67(17.9%)
			②	47	2	0/2 (0%)	0/45 (0%)
			③	55	1	1/1(100%)	7/54 (13.0%)
Ppa-tax-2	0.5	-	①	48	1	0/1 (0%)	0/47 (0%)
Ppa-tax-2	0.25	+	①	36	1	0/1 (0%)	0/35 (0%)
			②	22	1	0/1 (0%)	0/21 (0%)
Ppa-tax-2	0.62	+	①	2	1	1/1 (100%)	0/1 (0%)
			②	15	2	1/2 (50%)	0/13 (0%)
Ppa-tax-4	0.25	-	①	78	3	2/3 (66.7%)	14/75 (18.7%)
			②	3	1	0/1 (0%)	1/2 (50%)
			③	47	1	0/1 (0%)	0/46 (0%)
			④	22	2	0/2 (0%)	0/20 (0%)
Ppa-tax-4	0.5	-	①	73	2	0/2 (0%)	7/71(9.9%)
			②	34	1	0/1 (0%)	0/33 (0%)
Ppa-tax-4	0.62	-	①	74	1	0/1 (0%)	3/73 (4.1%)
Ppa-tax-4	0.62	+	①	43	10	10/10 (100%)	6/33 (18.1%)
			②	19	1	0/1 (0%)	2/18 (11.1%)